Genetic Diversity and Metamorphosis of White Wax Scale Insects

Genetic Diversity and Metamorphosis of White Wax Scale Insects

By

Hang Chen, Qin Lu, Xiaofei Ling, Jinwen Zhang, Weifeng Ding, Ni Liu, Pengfei Liu, Weiwei Wang and Juan Liu

Cambridge Scholars Publishing

Genetic Diversity and Metamorphosis of White Wax Scale Insects

By Hang Chen, Qin Lu, Xiaofei Ling, Jinwen Zhang, Weifeng Ding, Ni Liu, Pengfei Liu, Weiwei Wang and Juan Liu

This book first published 2023

Cambridge Scholars Publishing

Lady Stephenson Library, Newcastle upon Tyne, NE6 2PA, UK

British Library Cataloguing in Publication Data
A catalogue record for this book is available from the British Library

ISBN (10): 1-5275-9164-6
ISBN (13): 978-1-5275-9164-6

CONTENTS

PROLOGUE

Scale insects are hemimetabolous with incomplete metamorphosis and no true pupal stage. *Ericerus pela*, commonly known as the white wax scale insect (WWS), is a wax-producing insect found in Asia and Europe. The white wax, secreted by the male white wax insect as a kind of natural macromolecular compound, is an important industrial raw material and renewable resource. The main component of white wax is hexacosanyl ester of docosanoic acid. The wax is widely used in the machinery, chemical, medicine and other industries. The female is hyperpaurometamorphic, without wax secretion and wing forming, whereas the male has complete metamorphosis development with wax secretion only in the larva stage and wing formation in the adult stage. At present, the molecular mechanism of sexual dimorphic development of the white wax insect is still unclear, and effective ways to stimulate the insects to secrete more wax have not yet been found. This has become the long-standing problem and bottleneck in white wax industry development throughout the world.

The molecular mechanism of the development differentiation between male and female white wax insects will be revealed in this book. The book will contribute to the scientific support for improving wax production and promoting the development of the white wax industry. Our book is divided into five chapters, supported by specific biological evidence, research status and development trends, as well as a large number of charts and supporting information for the reader's reference. In Chapter 1, the genetic diversity and variability of nineteen different geographical populations are assessed to indicate that Southwest China is the original center of WWS, supported

by multiple gene evidence. The question how the regulation pattern of juvenile hormone and ecdysone in WWS affects sexual dimorphism development is explored in Chapter 2. The role of the ecdysone-induced *Ftz-F1* nuclear receptor transcription in the coordination of WWS growth and maturation is presented in Chapter 3. In Chapters 4 and 5, we use the high-quality data of whole genome and methylome analysis of the white wax scale insect to discuss the evolution of insect metamorphosis. Our book is a systematic, in-depth reflection of the latest research progress into the white wax scale insect. It provides new insights into the evolution of metamorphosis and sexual dimorphism in the scale insect. This book will afford interesting information for scientific and technical personnel, undergraduates, and graduate students engaged in entomology, molecular biology, and biogeography.

The research for this book was supported by grants from the Innovative Team of Yunnan Province (202005AE160011), the National Natural Science Foundation of China (31772542), and special grants for high-level overseas experts introduced to Yunnan province (YNQR-GDWG-2019-011). Limited by the author's ability and working conditions, this book has inevitable deficiencies. Therefore, we sincerely look forward to corrections and suggestions from scientists in entomology and molecular biology.

Dr. Hang Chen
in Edmonton, Canada
2022.1.12

CHAPTER 1

GENETIC DIVERSITY AND VARIABILITY IN DIFFERENT POPULATIONS

JINWEN ZHANG, JUAN LIU, WEIFENG DING, HANG CHEN

Abstract: The white wax scale insect (WWS) is a wax-producing resource insect found in Asia and Europe with high commercial value. The present study focuses on assessing the genetic diversity and variability in nineteen different populations of WWS collected from seven provinces around China. The amplified fragment length polymorphism technique was used to generate DNA fingerprints of individuals from each population. The percentage of polymorphic loci was 85.29%. Nei's genetic diversity and the Shannon index indicated that the Sichuan population is the highest followed by Yunnan, whereas Zhejiang was the lowest. High GST values among all sampled populations indicate a low degree of genetic variability within the population (40.85%) and higher variation among populations (59.15%). Nm values were low in all samples, suggesting low gene flow from events such as interbreeding and migration. Low gene flow values also suggest that populations of WWS become genetically heterogeneous due to counteracting forces such as strong differential selection. Our data support the theory that WWS will most likely remain localized and have a low potential to spread beyond their current habitats. The combined molecular phylogeny of nineteen WWS populations was generated using of *EF1a*, *SSU* and *COI* gene loci. The phylogenetic tree concluded that nineteen

different geographical populations of WWS are clustered into two groups, suggesting the origin centers of WWS. The Yunnan and Sichuan populations are mostly located at the base branch as primitive populations. It indicates that Southwest China is the original center of WWS with a high degree of bootstrap support.

Keywords: White wax scale insect, genetic diversity, gene flow, molecular phylogeny, origin center

1. Introduction

White wax scale insects (WWS, Hemiptera: Coccoidea), *Ericerus* pela Chavannes, an important resource insect, have been reared as a renewable bioresource for over a thousand years (Chen *et al*., 2021). Male WWS larvae secrete a white waxy substance that is increasingly utilized in many industries such as printing, medicine, food, chemical and machinery (Chen *et al*., 2011). WWS are widely distributed in the subtropic and temperate regions of Japan, Russia, and China (Figure 1) (Chen *et al*., 2021). The main ecological characteristics for suitable growth areas of *E. pela* are described as an annual average temperature of 11–16 ℃, light 1900–2500 h/a, rainfall 800–1200 mm, and an annual relative humidity of 65–75% (Chen *et al*., 2007). It is reported that the amount of wax excretion of the Kunming and Zhaotong populations is higher than other regions around China. The Chinese privet (*Ligustrum lucidum*) and Chinese ash (*Fraxinus chinesis*) are both excellent hosts of WWS (Figure 2), allowing the harvesting of more wax than that from other host plants (Chen *et al*., 1998; Chen, 2011).

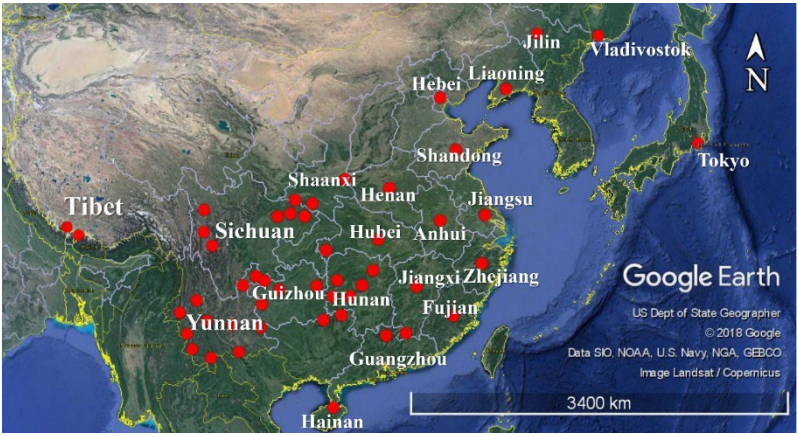

Figure 1 Distribution map of WWS in China, Japan, and Russia. The red points represent different locations with WWS distribution (Chen *et al*., 2021).

The transcriptome analysis of WWS during peak wax secretion provided an overview of gene expression information at the transcriptional level. Five genes related to white wax biosynthesis were identified, including *far* and *ws* (Yang *et al*., 2012). Genetic diversity is a vital factor to the sustainability in different populations (Hamrick *et al*., 1991). For the investigation of a species, knowledge of intraspecific genetic variations may help to assess inbreeding and evolutionary potential in a changing environment. To our knowledge, the genetic diversity and variability within and among populations of WWS has not been full researched until now. Furtherly, lack of any data supporting an assessment of whether the development of white wax insect industry will bring ecological imbalance has caused many controversial debates.

In this chapter, we used amplified fragment length polymorphism and combined gene sequencing to study the genetic composition and phylogeny among 19 populations of WWS (Table 1). The objectives of this study were:

1) to examine the genetic diversity and genetic variability in different WWS populations, 2) to assess the potential risk of diffusion for WWS in their natural habitats, and 3) to explore the phylogenetic relationships among populations to infer the original center of WWS and its diffusion route.

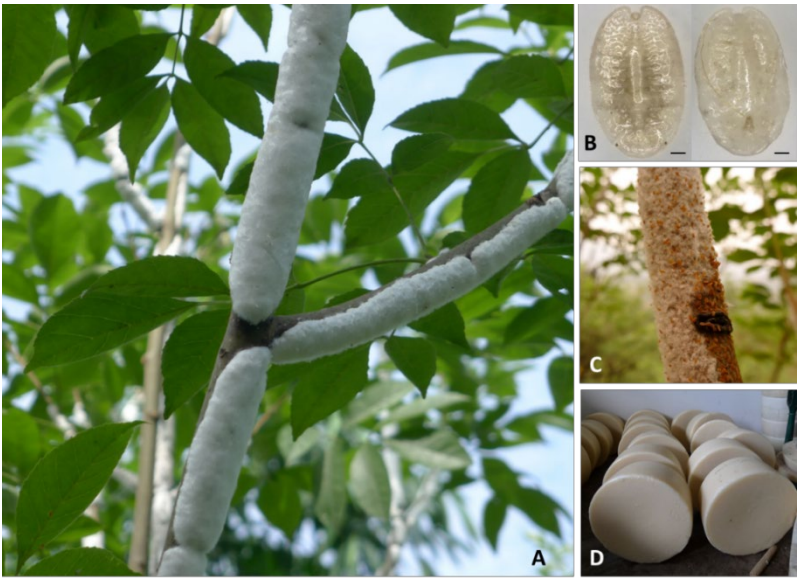

Figure 2 WWS producing white wax on its host tree. **(A)** WWS and its host tree *L. lucidum*; **(B)** The front and back view of WWS in the first larvae stage. The bar represents 30 μm; **(C)** WWS begin to secrete white wax in the second larvae stage after feeding on the branch of the host tree; **(D)** The products of refined wax made from white wax.

Table 1 Locations of different populations of WWS

No.	Location	Code	No.	Location	Code
1	Sichuan, Jinkouhe	JKH	11	Yunnan, Kunming	KMDB
2	Sichuan, Guangyuan	SCGY	12	Yunnan, Zhaotong	YNZT
3	Sichuan, Leshan	SCJK	13	Yunnan, Jianshui	YNJS
4	Sichuan, Emei	EMQL	14	Zhejiang, Hangzhou	HZTHA
5	Sichuan, Xide	XD	15	Jining, Changchun	JLCC
6	Yunnan, Dashiba	KMDS	16	Liaoning, Shenyang	LNSY
7	Yunnan, Guangji	JNGJ	17	Guizhou, Jinsha	GZJS
8	Yunnan, Yuxi	YXDB	18	Guangxi, Rongjiang	GLRJ
9	Yunnan, Chenggong	CGSC	19	Hunan, Suining	HNSN
10	Yunnan, Anning	KMAN			

2. Genetic diversity and variation

Twenty individuals from each population that produced banding patterns using all nine primer pairs were used in the analysis. The nine primer combinations used to analyze the 140 individuals from the 7 populations of WWS generated a total of 435 polymorphic loci, with their fragment sizes ranging from 200–1000 bp and the high polymorphic percentage 85.29% as an average value (Table S1). Also, the levels of polymorphisms that were observed within each population ranged from 2.55% for the Zhejiang population to 73.77% for the Sichuan population (Table 2). By analysis of Nei's genetic diversity (Nei, 1973) and the Shannon index on the seven populations of WWS, the two indices demonstrated the consistency of the results (Table 2). Nei's genetic diversity index was 0.01–0.30, in which the Sichuan population was the highest followed by the Yunnan population, while the Zhejiang population scored the lowest. Shannon's diversity index was 0.01–0.44, in which Sichuan population was still the highest followed

by the Yunnan population, whereas the Zhejiang population was the lowest in genetic diversity (Chen *et al*., 2015).

Table 2 Nei's genetic diversity and Shannon diversity index of WWS populations

Population ID	Polymorphic loci	Polymorphic Proportion (%)	Nei's Genetic Diversity Index (mean±SD)	Shannon Diversity Index (mean±SD)
Sichuan	373	73.33	0.30±0.20	0.44±0.28
Guizhou	80	15.69	0.07±0.15	0.09±0.22
Yunnan	282	55.29	0.22±0.21	0.32±0.30
Hunan	90	17.63	0.07±0.16	0.11±0.23
Zhejiang	13	2.55	0.01±0.06	0.01±0.09
Shanxi	77	15.10	0.06±0.15	0.09±0.22
Guangxi	67	13.14	0.05±0.14	0.08±0.20
All	435	85.29	0.27±0.17	0.42±0.24

The total genetic variance, measured as population heterozygosity (Ht), revealed a high genetic diversity value of 0.2473 among populations. Genetic variation within and among populations was measured as GST. The higher GST values (> 0.5) indicate that a majority of the genetic variability resides between populations. In our study, GST values among all sampled populations were high (0.5915), indicating a low degree of genetic variability within populations (40.85%) and high variation among populations (59.15%). Gene flow is commonly measured as Nm. Nm values beyond 1 indicate a high level of gene flow and the effects of gene flow on population differentiation is higher than the effect of random genetic drift (Bossart *et al*., 1998). In the present study, Nm values were relatively low in all samples, suggesting that low gene flow from events such as interbreeding and migration was inefficient (Table 3) (Chen *et al*., 2015).

Low gene flow values also revealed that local populations will become genetically heterogeneous, since they are subjected to differential selection and other counteracting forces.

Table 3 Genetic differentiation coefficient and gene flow among WWS populations

No. of populations	Ht	Hs	Gst	Nm
7	0.2473	0.1010	0.5915	0.3454

Ht: total genetic variance; Hs: genetic variance within population; GST: genetic differentiation coefficient; Nm: gene flow.

3. DNA sequencing

To assess the evolutionary relationships among 19 populations of WWS collected from different habitats, the combined sequence data of elongation factor 1 alpha (*EF1a*), small subunit ribosomal RNA (*SSU*), and cytochrome c oxidase subunit I (*COI*) gene loci were sequenced and analyzed in this study. Total genomic DNA was isolated from the whole insect body using a standard phenol with chloroform extraction technique. PCR products were purified with the QIAquick PCR purification kit and then sequenced directly in both directionson a Beckman CEQ2000XL automated sequencer. The resulting sequences were assembled by using Bioedit version 7.0.5.3 and are deposited in GenBank. The accession numbers (KX380921–KX380942 for the COI gene, KX380943–KX380962 for the *EF1α* gene, KX380963–KX380985 for the *SSU* gene) are listed in Table 4.

Table 4 Basic information of the 19 populations and accession numbers of three genes

NO.	Voucher Number	GenBank Accession No.		
		COI	***EF1α***	***SSU***
1	CGSC	KX380921	KX380943	KX380963
2	EMQL	KX380922	KX380944	KX380964
3	GLRJ	KX380923	KX380945	KX380965
4	GZJS	KX380925	KX380956	KX380966
5	HNSN	KX380926	KX380947	KX380980
6	HZTH	KX380927	KX380948	KX380981
7	JKH	KX380928	KX380953	KX380982
8	JLCC	KX380929	KX380957	KX380969
9	JNGJ	KX380930	KX380949	KX380970
10	KMAN	KX380932	KX380950	KX380972
11	KMDB	KX380933	KX380951	KX380974
12	KMDS	KX380934	KX380954	KX380973
13	LNSY	KX380935	KX380958	KX380975
14	SCGY	KX380937	KX380955	KX380977
15	SCJK	KX380938	KX380959	KX380978
16	SCXD	KX380939	KX380960	KX380986
17	YNJS	KX380940	KX380961	KX380983
18	YNZT	KX380941	KX380952	KX380984
19	YXDB	KX380942	KX380962	KX380985

The sequence characteristics for the three genes are shown in Table 5, as are combined gene data. Comparisons of the datasets revealed that mitochondrial sequences of *CO1*, with the largest proportions of variable (52.5%) and AT bias (62.9%), had a larger composite likelihood distance (about 6 times on average) than those in nuclear and combined genes. Among the two nuclear gene regions, *EF1a* showed the higher percentage

of variable and parsimony informative sites, though the mean ratio of transition and transversion was similar to *SSU*. In addition, the estimations of sequence divergences were larger for *EF1a* than for *SSU*.

Table 5 Characteristics for nuclear and mitochondrial sequences data

Dataset	C	V	S	Pi	Total (bp)	AT %	ti/tv	D-ML
EF1a	950	304 (22.4%)	342	38 (2.8%)	1356	59.5	1.3	0.058
SSU	537	50 (8.4%)	49	1 (0.2%)	592	47.0	1.5	0.012
CO1	279	353 (52.5%)	348	3 (0.4%)	673	62.9	1.1	0.364
Combined genes	1766	745 (28.4%)	701	42 (1.6%)	2627	57.4	1.2	0.063

C: conserved site; S: singleton; V: variable site; Pi: parsimony informative site; ti/tv: the mean ratio of transition and transversion; D-ML: overall average distance of different populations in maximum composite likelihood.

4. Phylogeny

The phylogenetic tree generated for the 19 populations of WWS based on combined *EF1a*, *COI*, and *SSU* gene data of 2627 bp sequences is show in Figure 3. The topologies resulting from maximum parsimony (MP) and maximum likelihood (ML) analyses are similar overall, supported by high bootstrap values varying for different branches with *P. comstocki* as an outgroup. The T92+G model was selected as the best model for phylogenetic analysis in accordance with the HLRT test (-In L = 5908.26) with the lowest BIC scores in constructing the maximum likelihood tree (Table S2).

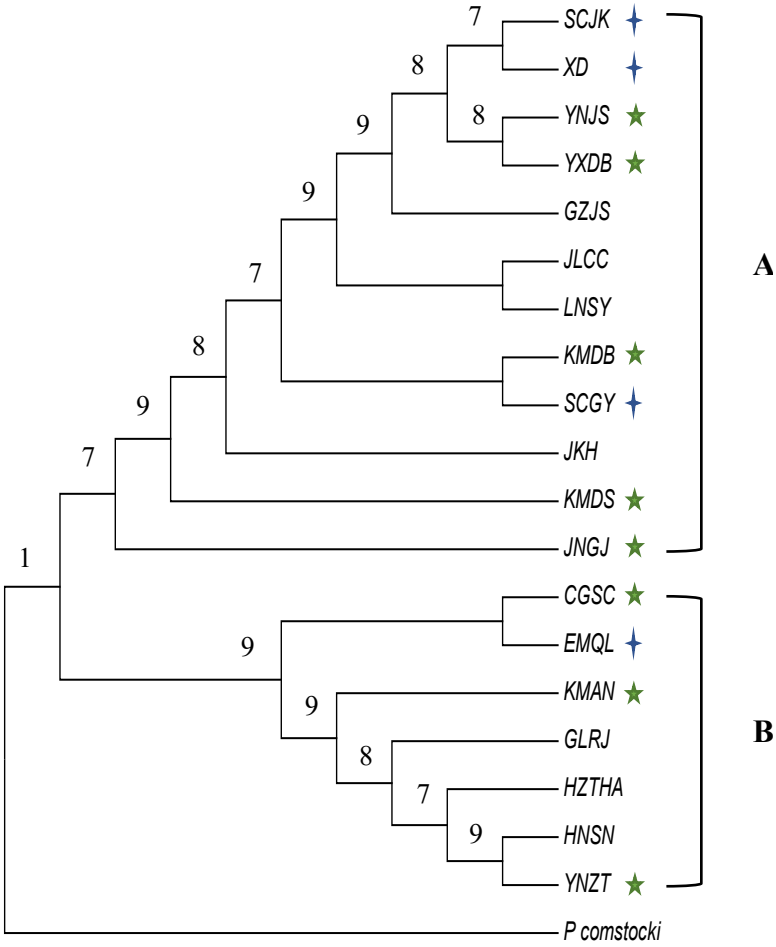

Figure 3 Phylogenetic tree of 19 populations of WWS based on combined analysis of *CO1*, *EF1a*, and *SSU* gene loci. MP consensus tree resulting from mixed-model and ML analysis of aligned 2629 bp (model = T92 + G) of combined genes from 19 populations from different geographical locations and combined species from related families as outgroup taxa. Numbers above internodes indicate MP bootstrap. The populations from Sichuan province are marked as blue stars and Yunnan populations marked as brown pentastars.

From the phylogenetic tree, it is concluded that the 19 different geographical populations of WWS are clustered into two groups, A and B. The findings suggest that there might be two origin centers of WWS with high bootstrap support. In group A, two populations (*JNGJ* and *KMDS*) from Yunnan province were more closely related to the outgroup taxa belonging to the primitive population of WWS. In group B, one population (*CGSC*) from Yunnan province and one population (*EMQL*) from Sichuan province were clustered as a sister group and located at the base branch as primitive populations. This indicates that Southwest China (including Yunnan and Sichuan) is the original center of WWS, and the diffusion trends of WWS occurred from west to east and from south to north in China.

5. Conclusion and Discussion

The silkworm, honeybee and WWS are the main three resource insects that have provided significant commercial benefits to humans for over thousands of years. The genetic background of both honeybee and silkworm have been sequenced and extensively annotated, whereas high quality genomic data among populations for WWS is still lacking (Chen *et al*., 2021). In this study, our data showed there are large differences in the tested polymorphic loci among populations of WWS. The polymorphic percentage of the Sichuan and Yunnan populations were 73.33% and 55.29%, respectively, much higher than those of other populations. For the genetic diversity index, the Sichuan population were highest followed by the Yunnan population. Shannon's diversity index was in the range of 0.01–0.44, with Sichuan and Yunnan being ranked highest two populations. This indicates that Yunnan and Sichuan possible represent the original center with so much higher genetic diversity than that in other populations.

In this study, GST values among the nineteen populations were high, indicating a low degree of genetic variability and high variation between

populations. These results show that there is plenty of genetic differentiation among the nineteen populations. The abundance of genetic differentiation among populations is generally considered the result of insufficient gene flow, coupled with selective pressures as well as genetic drift. Since all the WWS samples were collected from different locations with different environments, there should be a correlation between geographical isolation and genetic differentiation. Gene flow is commonly measured as Nm, where N is the number of individuals in a population and m is the proportion of individuals in the population as a result of immigration (Chandra *et al*., 2011). In the present study, Nm values were as low as 0.3454 in the tested regions, suggesting low gene flow of WWS from factors such as lack of interbreeding and migration. Low gene flow values also indicate that subpopulations will become genetically heterogeneous due to a range of counteracting forces such as strong differential selection. The low gene flow is possibly closely related with the poor diffusion ability of WWS. Together with the results on genetic diversity and variation, it is concluded that WWS populations will likely remain localized, and that there is only a low risk that any population will spread beyond its current habitat. This is possible the reasonable answer why the WWS has not been reported to cause any damage to forests or crops, despite the insect being raised in China and east Asia as a natural bioresource for thousands of years.

Our phylogenetic analyses indicate that the primitive populations, mostly from the Yunnan and Sichuan provinces, clustered in basal branches. The evolution trend of the WWS indicates that Southwest China (including Yunnan and Sichuan) is the center of origin of WWS (Fig. 3). Furthermore, Southwest China, with more than twelve populations, has the highest diversity of WWS of any region.

References

Bossart JL, Prowell DP. Genetic estimates of population structure and gene flow: limitations, lessons and new directions. Trends in Ecology & Evolution, 1998, 13(5): 202-206.

Chandra A, Reinert JA, LaMantia J, Pond JB, Huff DR. Genetic variability in populations of the southern chinch bug, *Blissus insularis*, assessed using AFLP analysis. Journal of Insect Science, 2011, 11(1): 1-10.

Chen H, He R, Wang ZL, Wang SY, Chen Y, Zhu ZC, Chen XM. Genetic diversity and variability in populations of the white wax insect *Ericerus pela*, assessed by AFLP analysis. Genetics and Molecular Research, 2015, 14(4): 17820-17827.

Chen H, Lu Q, Chen XM, Ling XF, Liu PF, Liu N, Wang WW, Zhang JW, Qi Q, Ding WF, Zhang X, Feng Y, Zhang YR, Chen MS, King-Jones K. Genome assembly and methylome analysis of the white wax scale insect provides insight into sexual differentiation of metamorphosis in hexapods. Molecular Ecology Resources, 2021, 21(6): 1983-1995.

Chen XM. Natural population ecology of *Ericerus pela*, Science Press, Beijing, 2011.

Chen XM, Chen Y, Ye SD, Wang SY, Wang ZL. Studies on wax secretion of Chinese white wax scale (*Ericerus pela*): Comparison on wax secretion of different geographic varieties. Forest Research, 1998, 11(1): 35-38.

Chen XM, Wang ZL, Chen Y, Ye SD, Wang SY, Feng Y. The impact of environmental factors on the wax excretion by Chinese white wax scale. Acta Ecologica Sinica, 2007, 27(1): 103-112.

Hamrick JL, Godt MJW, Murawski DA, Loveless MD. Correlations between species traits and allozyme diversity: implications for conservation biology. Genetics and conservation of rare plants, 1991, 3: 30-30.

Nei M. Analysis of gene diversity in subdivided populations. Proceedings of the national academy of sciences, 1973, 70(12): 3321-3323.

Yang P, Zhu JY, Gong ZJ, Xu DL, Chen XM, Liu WW, Lin XD, Li YF. Transcriptome analysis of the Chinese white wax scale *Ericerus pela* with focus on genes involved in wax biosynthesis. Plos One, 2012, 7(4): e35719.

CHAPTER 2

REGULATION PATTERN OF JUVENILE HORMONE AND ECDYSONE TO SEXUAL DIMORPHISM DEVELOPMENT

NI LIU, XIAOFEI LING, WEIWEI WANG, HANG CHEN

Abstract: The white wax scale insect (Ericerus pela, WWS) is a resource insect that is sexually dimorphic. The juvenile hormone (JH) and ecdysone (20E) titers and the expression patterns of hormone-related genes were measured at different developmental stages. The results showed that JH and 20E cooperate to regulate the development of WWS and that the titer of JH was higher in females than in males during the whole growth period. The first nymph is the starting point of dimorphic development, and the low concentration of JH induces the complete metamorphosis of the males. There is a certain amount of titer difference when 20E antagonizes JH, and when the difference between JH and 20E titer was between 31.019 and 59.366 pg/mg, both males and females could develop normally. Real-time quantitative (qPCR) results indicate that *FPS*, *FDS*, and *PMVK* genes in the JH signaling pathway are only highly expressed in the female second-instar nymph. *JHAMT* and *FAMeT* genes are only highly expressed in the male second-instar nymph. *FPS*, *FDS*, *PMVK*, *JHAMT*, and *FAMeT* are putative key genes involved in the development of sexual dimorphism. The expression trend of the *MeT* gene, the encoding JH receptor protein, was opposite to the change of JH titer in females, and its expression trend in

males was consistent with the change of JH titer. However, the expression changes of *EcR*, the encoding ecdysone receptor protein, were consistent with the changes in 20E titer in both females and males. The results indicate that the receptor protein *MeT* was regulated negatively by JH in females but positively in males, while 20E positively regulates the expression of the *EcR* gene encoding its receptor protein in both females and males. The effects of artificially controlled spraying of exogenous juvenile hormone analogs (JHA) on the synthetic genes of JH and 20E signaling pathways were different in time. JH2 (2.5 mg/mL) could up-regulate the expression of the *MeT* gene, combining the effects of JH2 on the wax secretion and the increasing trend of JH titer in the early stage of the second-instar male nymph. JH may shorten the time to reach the peak of the secretion of wax or extend the development for the second-instar male nymph. These findings afford a new understanding of the development of hormone-regulated genes and provide new insight into the evolutionary trend of insect metamorphosis.

Keywords: *Ericerus pela*; sexual dimorphism; ecdysone; juvenile hormone analogs (JHA); gene expression pattern

1. Introduction

Juvenile hormone (JH) and ecdysone (20E) regulating insect molting and metamorphosis have been reported in most metamorphic insects (Yamanaka *et al*., 2013; Nijhout *et al*., 2014). JH, secreted by the insect pharynx as a sesquiterpene controls metamorphosis, reproduction, diapause, and many other developmental processes of insects (Nijhout, 1994). 20E, produced by the prothoracic gland, controls the transition of each important developmental stage in the insect's life cycle (Thummel, 2001). The biosynthesis and metabolism of JH and 20E have been studied extensively in *Drosophila*, *Bombyx mori*, and others (Elekonich *et al*., 2003;

Parthasarathy, 2009). Acetyl coenzyme A is catalyzed by a series of enzymes and forms JH (Bede *et al*.,2001; Minakuchi and Riddiford, 2006; Kinjoh *et al*., 2007). There are some specific enzymes involved in JH biosynthesis, such as HMGR, FPS, and FAMeT (Fig. S1). The spatial-temporal characteristics of JH titer are regulated by both synthesis and metabolism. JH metabolizing enzymes include juvenile hormone esterase (JHE), juvenile hormone epoxide hydrolase (JHEH), and juvenile hormone diol kinase (JHDK) (Li *et al*., 2004). Due to the lack of squalene, insects cannot de novo synthesize 20E, but cholesterol or phytosterols from foods provide precursors for 20E synthesis (Sakurai and Gilbert, 1990). The biosynthetic pathway of 20E is mainly catalyzed by the hydroxylase encoded by the cytochrome P450 family genes (*CYP302A1*, *CYP306A1*, *CYP307A1*, *CYP314A1*, and *CYP315A1*) and forming 20-Hydroxydeciduone with activity (Gilbert, 2004; Gilbert and Warren, 2005; Yurika *et al*., 2011). JH, a hydrophobic sex hormone, does not act directly on the target cells. Methoprene-tolerant protein and taiman (*tai*), the protein partner of MeT, convey the JH signal to prevent precocious metamorphosis, and the functional molting hormone receptor consists of the products of EcR and ultraspiracle (*usp*) (Vlastimil *et al*., 2014; Yang *et al*., 2015; Nakagawa and Henrich, 2009).

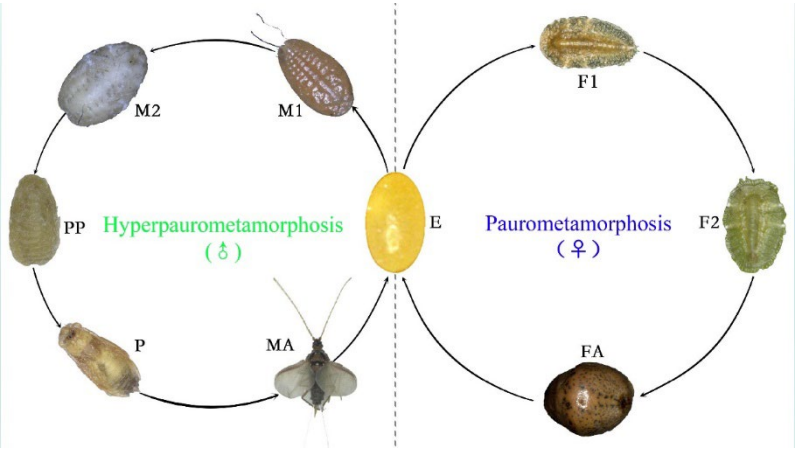

Figure 1 Female and male life history of *Ericerus pela*. The females develop through an egg (E), first-instar nymph (F1), second-instar nymph (F2), and adult (FA). The males develop through an egg (E), first-instar nymph (M1), second-instar nymph (M2), prepupa (PP), pupa (P), and adult (MA) (Chen *et al*., 2021)

Ericerus pela (*E. pela*), known as the white wax scale insect, has been bred in China for over a thousand years. It is mainly distributed in China, Japan, and Russia, from the subtropics to temperate regions. The wax secreted by the male larvae is a kind of pure natural raw material, which has been widely used in chemical, machinery, pharmaceutical, food, and other industries (Chen *et al*., 2009, 2021). Most of the white wax producers are distributed in poor mountainous areas, so the increasing yield of white wax can not only promote economic development in villages but also requires planting a large number of host plants, which has important ecological, economic, and social benefits. The white wax scale insect breeds one generation every year through parthenogenesis or sexual reproduction. It is a typical example of sexual dimorphism in insects. Females exhibit incomplete metamorphosis, developing through egg, first-instar nymph, and second-instar nymph to

adult, while males undergo complete metamorphosis through egg, first-instar nymph, second-instar nymph, prepupa, and pupa, finally to adult (Chen *et al*., 2011). Females and males display some differences in morphology, physiology, and behavior. Females enjoy light and find the sunny side of the host, whereas males are photophobic and gather in the shady side of the host to secrete wax to adapt to the environment, with two transitions in the life cycle of females and males (Fig. 1). There is a peak period of wax secretion in the second-instar male nymph, and it has been reported that far and *ws* genes are involved in the regulation of wax secretion in male nymphs (Yang *et al*., 2012; Chen *et al*., 2021).

However, how do JH and 20E participate in the regulation development of sexual dimorphism in insects? The interaction between JH and 20E at the biological and molecular levels has not been fully researched. So far, there is no clear understanding about the effect of juvenile hormone analogues (JHA) on the production of white wax. In order to promote the development of the white wax industry, the method and dose of JHA treatment are worthy of further study.

In this chapter, we will try to answer the following questions: 1) How do JH and 20E affect and regulate the development of white wax scale insects? 2) What are the key genes related to JH and 20E that regulate sexual dimorphism development? 3) What are the key gene expression patterns? The exogenous hormones were applied under artificial control conditions to analyze the stress response and gene expression patterns of white wax insects. All of these will help to explore the causes of the differentiation of sexual dimorphism of white wax insects and to reveal the internal rules of dimorphic metamorphosis in the species.

2. The titer regulation of JH and 20E during dimorphic development

The Chinese white wax scale insect is a typical example of sexual dimorphism in insects and displays differences in morphology, physiology, and behavior between females and males. At the egg stage, the eggs of both sexes coexist in insect seed bursa, and there is a small amount of wax filaments wrapped in them. However, it is easy to distinguish between female and male eggs at this time, since the female eggs have a darker, reddish-brown color and the male eggs have a paler, light-yellow color (Figs. 1 and 2A). At the first-instar nymph stage, female and male migrate on the first crawl and began to separate. At this time, the females are yellowish-brown and inhabit the upper sides of leaves along the veins, while their tentacles and feet are thick, and the tail silks are clearly visible (Figs. 1 and 2A). In contrast, the males are canary yellow and inhabit the lower surfaces of leaves with a small amount of wax, but their tentacles, feet, and tail silks are similar to those of the females (Figs. 1 and 2B). At the second-instar nymph stage, females and males undergo the second crawling and distribution along the limb, and they are flattened circular; their tentacles, feet, and tail silk are lost, but only the males secrete wax (Figs. 1 and 2B). Next, the female transition directly into the adult stage; they change little, with their shape remaining unchanged, but the cuticula keratinizes (hardens), body volume grows, and there is a deepening of color. After laying eggs, the horny shell gradually shrinks and dries (Fig. 1, FA). Males undergo prepupal and pupal stages, then the eclosion; their tentacles and tail silk become longer. Male adults have wings and can fly (Fig. 1, MA).

Over the whole life cycle of the female and male, the change trend of JH titer was basically consistent and showed a downward trend from nymph to adult, and at the adult stage, there was almost no JH detected (Fig. 2A, 2B, and Fig. S2). The titer of JH was higher in females (incomplete

metamorphosis) than in males (complete metamorphosis) during the whole growth period (Fig. 2C). For the titer of 20E, males were higher than females from first-instar nymph to the early stage of second-instar nymph, and females in the adult stage were relatively high (Fig. 2D). At the middle of the first-instar stage, the titer of JH showed a peak appearing, the female JH titer was approximately 10-fold that of the male (female: 91.640 pg/mg; male: 8.980 pg/mg), and for the time of reaching the peak, the female was late (Fig. 2C). After the second-instar larvae of females, the JH titer was significantly higher than that of 20E, while from nymph to adult, the 20E titer of males was always higher than JH, and the fluctuation of titer was larger than that of JH (Fig. 2A and 2B).

During the developmental transition period, the titer of JH showed a trend of gradually decreasing and had a lower value (0.941 ~ 10.026 pg/mg). However, the 20E titer showed the opposite trend with JH (M1 shows a downward trend) and had a higher value (33.856 ~ 82.972 pg/mg). The difference in the titers of JH and 20E was from 23.830 to 79.749 pg/mg in females and 31.019 to 59.366 pg/mg in males (Fig. 2A and 2B). In addition, 20E showed a trend of wave-like change in the male prepupa and pupal stages, and there were three peaks of similar size (Fig. 2B). At the adult stage, the titer of 20E appeared to be the highest, of which the female 20E titer was about 26 times that of the JH (20E titer：82.972 pg/mg; JH titer: 3.223 pg/mg), and the male 20E titer was about 40-fold that of the JH (20E titer：60.822 pg/mg; JH titer: 1.456pg/mg) (Fig. 2A and 2B). At this time, male and female JH titers were small and comparable in size (female: 2.0419 pg/mg; male: 1.386 pg/mg), and male and female 20E titers differed by 18.456 pg/mg (Fig. 2A and 2B).

In summary, the changes of JH and 20E titers have the same patterns and differences in females and males, and at the transition period, 20E

antagonizes JH with a precise titer change to regulate the development of females and males.

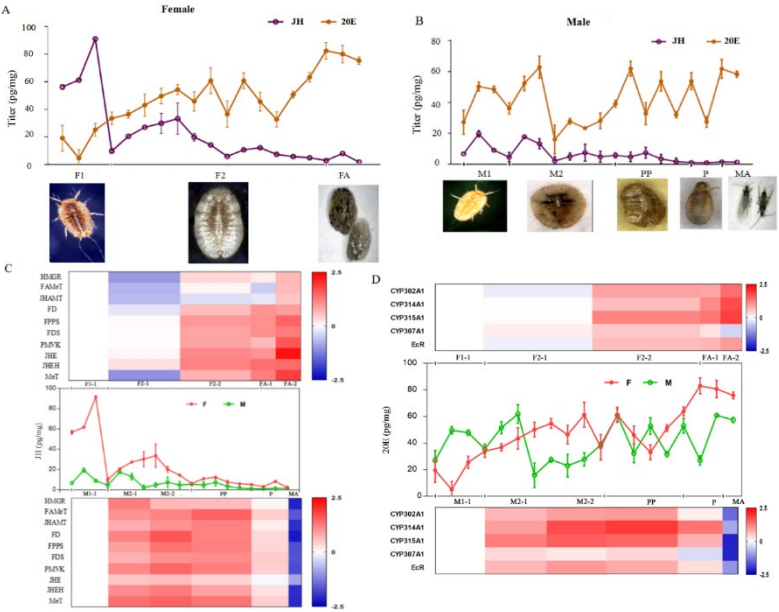

Figure 2 The change of JH and 20E titer with the expression pattern of related genes in different development stages. Gene expression is conversed by Log_{10}. The expression level is between -2.5 and 2.5, with 0 as the benchmark line. The morphology and JH and 20E titer in the different development periods of female (**A**) and male (**B**) *E. pela*. The X-axis represents different development periods of females (**A**) and males (**B**). The Y-axis represents the titer level of JH (left) and 20E (right). The line charts show the titer of JH (**C**) and 20E (**D**) in different development periods. The X-axis represents different development periods of females (top) and males (bottom). The Y-axis represents the titer level. The expression level of JH (**C**) and 20E(**D**) related genes in different development stages are displayed on the top (female) and bottom (male) of the heat map.